Charge transfer $Cr^{3+}(3d^3) \rightarrow Cr^{2+}(3d^4)$ in chromium-doped GaAs

G. Martinez, A. M. Hennel,* W. Szuszkiewicz,* and M. Balkanski
Laboratoire de Physique des Solides associé au Centre National de la Recherche Scientifique, Université Pierre et Marie Curie, 4 place Jussieu, 75230 Paris Cedex 05, France

B. Clerjaud
Laboratoire de Luminescence II, Equipe de Recherche associée au Centre National de la Recherche Scientifique, Université Pierre et Marie Curie, 4 place Jussieu, 75230 Paris Cedex 05, France

(Received 7 July 1980)

Results on the absorption and electron paramagnetic resonance measurements on chromium-doped GaAs are reported. For p-type samples the main optical transitions are shown to be due to a photoionization process which has been measured as a function of temperature and hydrostatic pressure. A model, developed in the configurational diagram scheme and using two types of relaxation, is proposed to explain the experimental results.

I. INTRODUCTION

Whereas a number of luminescence studies have been performed on GaAs doped with chromium,[1-4] the absorption due to these impurities has received comparatively little attention.[5,6] In particular, no clear interpretation of the observed spectra has been afforded. This contrasts with the results on the same impurity in II–VI compounds where EPR results,[7] optical measurements[8,9] and their interpretation, now give a coherent picture of the physical situation.[9] One of the problems encountered with III–V compounds is that the limit of solubility of the chromium, for example in GaAs, is less than 10^{18} cm^{-3}, making all optical measurements more difficult. Another fact which obscures the field is the presence, besides the "normal" Cr^{3+} charge state, of the Cr^{2+} charge state and of an extra charge state assigned by most of the experimentalists to Cr^{1+} (Ref. 10) but which could be assigned as well to Cr^{4+} as was recently suggested.[11] These three charge states which have been recognized by EPR measurements,[10] can coexist in some samples, making the interpretation of the results (especially luminescence data) very delicate.

It is then clear that a more systematic study of samples in which the chromium concentration as well as the free-carrier concentration vary, while other impurity concentration remains constant, would help to clarify the problems. It is also important that these samples would be characterized by the largest number of techniques and especially by systematic EPR measurements in order to know what kind of charge states we are dealing with. This is the approach we have chosen. The doped samples can be classified into two groups; one for which the Cr^{2+} charge state is dominant and the electrical conduction remains n type, and the second for which the Cr^{3+} charge state is dominant and which are p type. We report here results on p-type samples, delaying those on n-type samples to a second paper,[12] hereafter referred to as paper II.

After the description of the preparation of the samples and the discussion of the results of the characterization procedures performed on them, we briefly present the experimental setup used for optical measurement under high pressure and for EPR measurements. The experimental results on the absorption of p-type samples as a function of temperature and pressure are shown. A theory of the photoionization cross section involving two types of phonons is then proposed and used to interpret and discuss the experimental results. The last section is devoted to a discussion of the different EPR signatures obtained on our samples with and without optical illumination.

II. PREPARATION OF THE SAMPLES

A GaAs ingot doped n type during the liquid phase growth has been used as the basic substrate for all chromium diffusions. This ingot was provided by the RTC Company (Caen, France). Slices of 3-mm thickness were cut from this ingot, polished, and chemically etched. Then chromium was evaporated under vacuum on both faces of the slab and each slab was diffused at different temperatures and different conditions which are recorded in Table I. Each face of the sample was then mechanically ground till a thickness of about 400 μm was eliminated, and then each sample was characterized by Hall-effect and EPR measurements.

As is shown on Table I, eight types of samples have been obtained and labeled Cr_0 to Cr_8. The Cr_0 sample which is not diffused has been analyzed by spark mass spectroscopy and secondary ion mass spectroscopy (SIMS). Both methods are able to reveal an iron concentration of about 5×10^{15} cm^{-3}. The donor impurities were detected as silicon in the range 8×10^{17} cm^{-3} and as tellur-

TABLE I. Conditions of preparation and results of characterization of the samples. The chromium concentrations marked with an asterisk have been deduced by the optical scaling of the intracenter absorption (see paper II).

	Diffusion temperature (°C)	Diffusion time (days)	Conduction type	Carrier concentration – 77 K (cm^{-3})	Mobility – 77 K ($cm^2 V^{-1} sec^{-1}$)	Chromium concentration (cm^{-3})
Cr_0			n	1×10^{18}	2400	
Cr_1	960	1	n	$\sim 6 \times 10^{17}$	2160	$*4 \times 10^{16}$
Cr_2	1100	1	n	$\sim 5 \times 10^{17}$	1500	$*4 \times 10^{16}$
Cr_3	1100	1	n	$\sim 3 \times 10^{17}$	1770	$*9 \times 10^{16}$
Cr_4	1130	1	n	$\sim 1.5 \times 10^{17}$	1170	$*1.8 \times 10^{17}$
Cr_5	1130	1	n	$\sim 1 \times 10^{17}$	1030	$*1.4 \times 10^{17}$
Cr_6	1100	3	n	$\rho \simeq 10^3$ Ω cm		9×10^{16}
Cr_7	1120	3	n	$\rho \simeq 10^7$ Ω cm		2×10^{17}
Cr_8	1150	3	p	$\rho \simeq 10^5$ Ω cm		3×10^{17}

ium in the range 8×10^{16} cm^{-3}. Aluminum is also found in the range 8×10^{16} cm^{-3}, whereas all other impurities are below $10^{15} cm^{-3}$. Besides the last sample (Cr_8), the results of which are reported here, all other samples remain n type and results of these will be reported in paper II. All samples have been diffused under vacuum except the Cr_2 sample for which an extra piece of Cr_0-GaAs was maintained in the same ampoule at a temperature 40 °C higher than that of diffusion. As can be seen in Table I, no drastic change has been detected from our characterization procedure. It turns out, however, that the time of diffusion is a dominant parameter although the chromium disappears rather quickly from the sample surface even after six hours of diffusion. So it is likely that the diffusion process has two important steps: a first one which allows the chromium to enter the sample probably along the dislocations, and then a slower one which is the real process of diffusion leading the chromium ion in a substitutional site of gallium.

Contacts were made with indium drops on the sample annealed at 250 °C under vacuum during twenty minutes. As can be seen in Table I, no correlation is found between the temperatures of diffusion, the mobility, and the compensation expected between the chromium, silicon, and tellurium impurities. Clearly a second compensation mechanism is present, probably due to As vacancies, and it is possible that the local homogeneity of the sample is not preserved, although optically it looks good.

The chromium concentration has been measured by SIMS and results are reported in Table I for the Cr_6, Cr_7, and Cr_8 samples. These measurements allow us to calibrate the different optical cross sections for the optical transitions, calibrations which in turn are used to determine the chromium concentration in samples Cr_1, Cr_2, Cr_4, and Cr_5. The EPR results will be presented, together with other experimental results for the samples and will be discussed in detail at the end of this paper.

III. EXPERIMENTAL SETUP

The absorption experiments at temperatures in the liquid-helium range were performed with a Jobin-Yvon HRS monochromator with a resolution of about 0.2 cm^{-1}. The detector was an uncooled PbS detector used in its linear range. The experimental assembly was swept with dry nitrogen in order to decrease the water-vapor absorption. A variable-temperature Air Liquide cryostat was used, the sample merging the liquid or gas helium depending on the temperature.

The absorption measurements under high pressure at 77 and 300 K were made using another assembly composed of a Coderg S 20 spectrometer followed by a cooled PbS detector. The resolution here is only of about 5 cm^{-1} but is still sufficient for the type of spectra we are measuring in this temperature range. All the assembly is maintained under a primary vacuum which eliminates the water-vapor absorption.

The high-pressure apparatus compressed the helium gas up to 10 kbars in an optical high-pressure optical cell made with maragin steel. This cell has four optical apertures with sapphire windows and can merge a nitrogen-liquid bath in a special cryostat. The use of helium gas preserves the hydrostaticity of the pressure up to 14.7 kbars at 77 K. Because of the precision required in the strength of the absorption coefficients (~0.02 cm^{-1}), we have been led to introduce in the high-pressure cell a system allowing in-out measurements *in situ* at all temperatures and pressures. This has been achieved by a small electrical engine which rotates the sample holder inside the high-pressure cell. The whole assembly will be described in a further publication.[13]

The EPR experiments have been performed with

a Varian V 4502 spectrometer equipped with an *X*-band microwave bridge constructed in the laboratory.[14]

A gas-flow Oxford instrument ESR 9 cryostat allows us to work at temperatures down to 3.5 K. This assembly is made in such a way that three concentric quartz tubes are introduced in a TE_{102} cavity. Because of the relatively high dielectric constant of quartz (~4), the microwave-field lines are strongly distorted in the cavity, allowing some electric-field lines to be perpendicular to the static magnetic field at the sample position. This induces cyclotron resonance effects which limit the observation of EPR signals for the samples of Table I with the highest carrier concentration.

IV. EXPERIMENTAL RESULTS

A. Absorption measurements

The absorption coefficient has been measured as a function of the temperature between 4.5 and 300 K and of the pressure up to 10 kbars at 300 and 77 K. The main characteristic of the spectrum is an asymmetric broad band extending over a few thousand of cm^{-1} and for which the low-energy tail is strongly temperature dependent. This structure is found in our *p*-type samples (Cr_8) and also in semi-insulating GaAs doped with chromium in the liquid phase as was already reported.[6,15,16] The comparison of the spectra obtained for these two types of chromium-doped GaAs is shown in Fig. 1 (the RTC sample has been provided by G. Poiblaud of the RTC Company, Caen, France). Within the experimental error these absorption spectra are proportional, indicating that the structure of the absorption does not depend on the method of preparation.

We shall now concentrate on the Cr_8 sample which is clearly the more doped sample in that series. Figure 2 shows the shape of the absorption at 4.5 K and two main features appear: the low-energy tail has varied significantly and a weak but clear additional structure is superimposed on the main spectrum.

Both these features are still present at liquid-nitrogen temperature and since at this temperature the pressure effect can be studied, we report in Fig. 3 at 77 K the measured variation of the absorption coefficient as a function of the pressure. This effect clearly does not change the shape of the spectrum and shifts only the onset of transitions towards higher energies.

B. EPR measurements

Part of the EPR spectrum of the Cr_8 sample is shown in Fig. 4. In the absence of a light excitation, the Cr^{3+} signal is clearly dominant whereas some residual Cr^{2+} state can be detected. The same spectrum recorded under the illumination of the 1.09-μm line of an argon laser is quite different and shows a charge transfer between the Cr^{3+} and Cr^{2+} charge states. This effect is reversible. Noticing that the 1.09-μm line corresponds to an energy of 9170 cm^{-1} which fits well the maximum of absorption in Figs. 1–3, we are then led to assume that this absorption is due to a charge transfer from Cr^{3+} to Cr^{2+}, also called a photoionization transition. This is the same kind of process seen

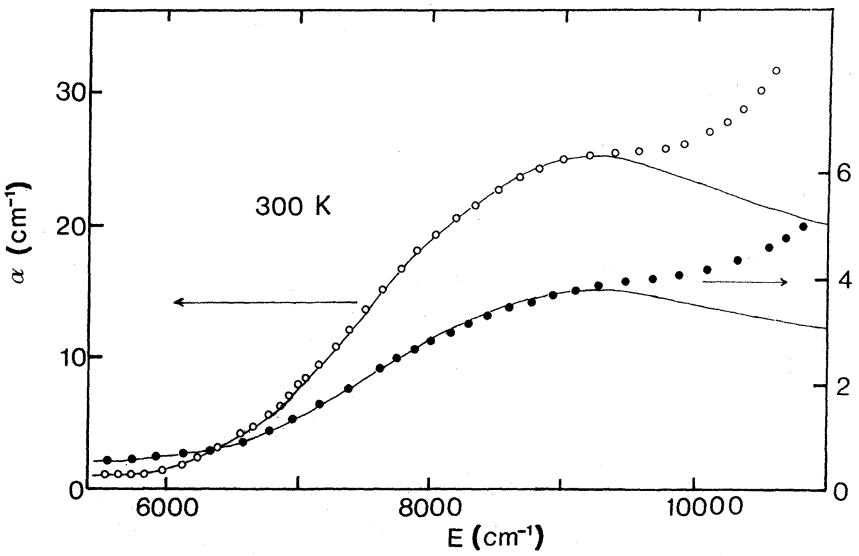

FIG. 1. Absorption spectra of the Cr_8 sample (empty dots) and RTC sample (full dots) at 300 K, as a function of the energy. The theoretical curves (full lines) are obtained by fitting Eq. (13) to the experimental points.

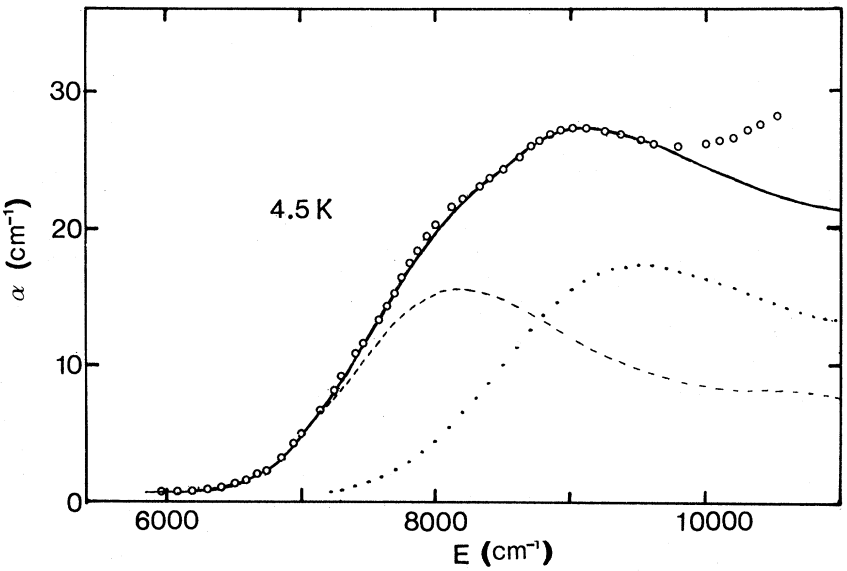

FIG. 2. Absorption spectrum of the Cr_8 sample (empty dots) at 4.5 K as a function of the energy. The dashed and dotted curves are the two contributions given by Eq. (13), the full line resulting in the sum of the two preceding curves.

in II–VI compounds doped with transition-metal impurities by Kaminska *et al.*[17] with the difference that the charge transfer occurs in this case between Cr^{2+} and Cr^{1+}. A similar effect was also reported by Piekara *et al.*[18] on CdF_2 doped with In, in which the process involved a transfer of an electron from the impurity towards the conduction band. So the nature of such transitions is well understood and the problems which arise are connected to the models used to reproduce the experiments qualitatively as well as quantitatively.

V. THEORY OF THE PHOTOIONIZATION SPECTRA

A. Vibrational coupling

Many papers have dealt with photoionization phenomena. They can be classified into two groups, the first one neglecting the phonons or assuming their effect to be negligible at low temperatures, and the second one trying to reproduce the temperature effects and then involving transitions between vibronic levels rather than between pure electronic levels. It turns out that for these tran-

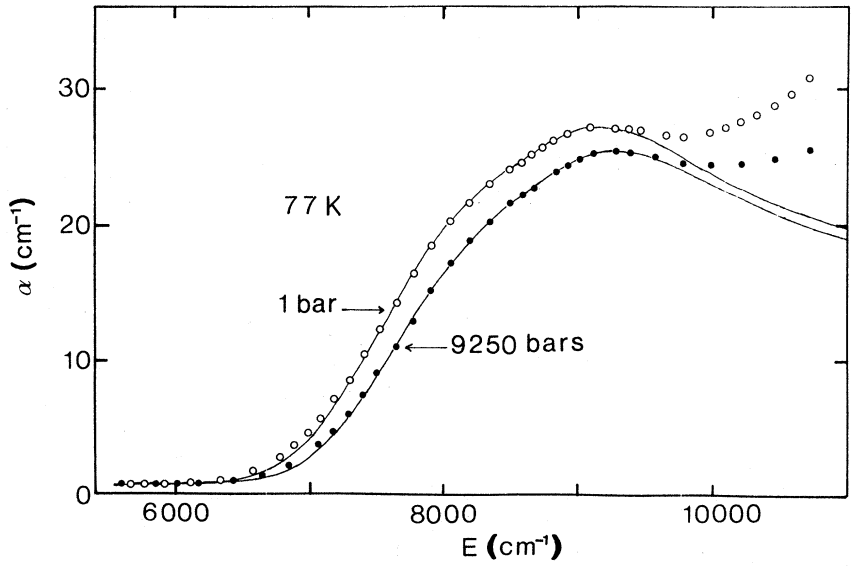

FIG. 3. Absorption spectra of the Cr_8 sample at 77 K, 1 bar (empty dots) and 9.25 kbars (full dots), as a function of the energy. The full lines are the results of the fitting of the theory [Eq. (13)] to experiments.

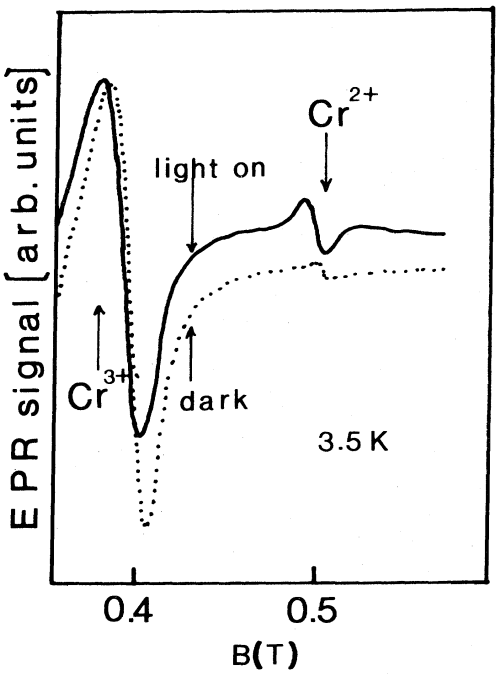

FIG. 4. Part of the EPR spectra of Cr_8 sample in the dark (dotted line) and under illumination with the 1.09-μm line of an argon laser (full line). These spectra are recorded with the configuration $\vec{B} \parallel [110]$ and at a frequency $f = 9.24$ GHz.

sitions the main effect is an emission of phonons in such a way that even at low temperatures they cannot be neglected. So, theories like those introduced by Allen[19] or Bebb[20] cannot really be fitted in their simple form to experimental curves. On the other hand, the concept of vibrational levels describing the initial and final states of the transitions appear to be well adapted to the description of experimental results. It was first introduced by Kopylov and Pikhtin[21] and then extended to the case of CdF_2 : In by Piekara *et al.*[18] and to that of ZnSe : Cr by Kaminska *et al.*[17] All these models postulating the Franck-Condon principle use the semiclassical approximation and assume a linear coupling between the electronic and vibrational part in the Hamiltonian describing the system. These models are restricted to one type of phonons which are taken as symmetric by the authors who assume for the electronic part of the matrix element a simple two-band model with similar effective masses. These last two assumptions are strongly reflected in the shape as well as the strength of the cross section in such a way that it is worth analyzing them in detail.

The cross section for transitions between an initial state $|i\rangle$ and a final state $|f\rangle$ is given by

$$\sigma(\hbar\omega) = \frac{\mathcal{C}}{\hbar\omega} A_i \sum_f |\langle f|\vec{p}|i\rangle|^2 \delta(\epsilon_f - \epsilon_i - \hbar\omega) . \quad (1)$$

The average A_i is understood to be an average over the initial vibrational states $|i\rangle$ with energy ϵ_i and the summation Σ_f extends over the final vibrational states $|f\rangle$ with energy ϵ_f. $\mathcal{C}$ is a constant which shall be specified below.

In our problem, the initial state is that of a valence electron (Γ_5 symmetry) besides a Cr^{3+} state in a $3d^3$ configuration, and the final state is that of the electron in the Cr^{2+} environment ($3d^4$ configuration). Krebs and Stauss have shown by EPR measurements[10] that both Cr^{3+} and Cr^{2+} were suffering a nonsymmetrical distortion due to a Jahn-Teller effect. However these distortions are not identical, Cr^{2+} being distorted along $\langle 100\rangle$ directions with a D_{2d} symmetry and Cr^{3+} along $\langle 1\bar{1}0\rangle$, $\langle 110\rangle$ and $\langle 001\rangle$ directions with a C_{2v} symmetry. Following the Franck-Condon principle, the electron is optically transferred to a state with a $3d^4$ configuration in an environment distorted like the stable configuration of Cr^{3+}. So physically, we expect at least two types of relaxation for the system: the first one which was taken into account by all the authors[17,18,21] is that induced by an additional Coulombic interaction which can naturally be reproduced with a symmetrical relaxation driven by A-type phonons and a second one driven by nonsymmetric phonons relaxing the system from a Cr^{3+}-like distortion to a stable Cr^{2+} one. We shall assume for the moment and discuss later on that this last distortion can be recovered by E phonons of the same type as those involved in the relaxation due to the Jahn-Teller effect for Cr^{2+}. It is shown in paper II that such phonons have an energy very close to that of the TA phonons of the host lattice in the X direction. Furthermore, if the Coulombic interaction is expected to be larger than the phonon interaction, there is no physical reason to think, *a priori*, that one relaxation is negligible before the other one. We shall then try to derive a model for which both relaxations are present.

The initial and final states are then described by a vibronic wave function which, with the Born-Oppenheimer approximation, can be written as

$$\begin{aligned} |i\rangle &= \psi_i \chi_p^A(Q_A)\chi_m^E(Q_\theta)\chi_n^E(Q_\epsilon) , \\ |f\rangle &= \psi_f \chi_r^A(Q'_A - Q_A)\chi_s^E(Q'_\theta - Q_\theta)\chi_t^E(Q'_\epsilon - Q_\epsilon) , \end{aligned} \quad (2)$$

where m, n, p, r, s, and t describe the different vibrational states of the standard harmonic oscillator function $\chi(Q)$, Q_A describing the distortion induced by an A phonon and Q_θ and Q_ϵ those by an E phonon. ψ_i and ψ_f are the electronic part of these wave functions.

Then the matrix element entering (1) is simply given by

$$|\langle f|\vec{\mathfrak{p}}|i\rangle|^2 = |\langle\psi_f|\vec{\mathfrak{p}}|\psi_i\rangle|^2 |\langle\chi_r^A(Q'_A - Q_A)|\chi_p^A(Q_A)\rangle|^2 |\langle\chi_s^E(Q'_\theta - Q_\theta)|\chi_m^E(Q_\theta)\rangle|^2 |\langle\chi_t^E(Q'_\epsilon - Q_\epsilon)|\chi_n^E(Q_\epsilon)\rangle|^2 .$$

Following Lax[22] and using the semiclassical approximation which assumes a large value of the excited vibronic state, each excited vibrational wave function, for example, $\chi_s^E(Q'_\theta - Q_\theta)$, is approximated by a δ-like function, $\delta(Q'_\theta - Q_\theta^s)$, and each matrix element $|\langle\chi_s^E(Q'_\theta - Q_\theta)|\chi_m^E(Q_\theta)\rangle|^2$ by $[\chi_m^E(Q_\theta^s)]^2$. Then expression (1) can be written

$$\sigma(\hbar\omega) = \frac{\mathfrak{C}}{\hbar\omega} A_i \int_{-\infty}^{+\infty} dQ_A^r \int_{-\infty}^{+\infty} dQ_\theta^s \int_{-\infty}^{+\infty} dQ_\epsilon^t \int_0^{+\infty} d\epsilon\, \rho(\epsilon) M^2 [\chi_p^A(Q_A^r)\chi_m^E(Q_\theta^s)\chi_n^E(Q_\epsilon^t)]^2 \delta(\epsilon_f - \epsilon_i - \hbar\omega) , \tag{3}$$

where $\vec{M}$ is the electronic dipole matrix element $\langle\psi_f|\vec{\mathfrak{p}}|\psi_i\rangle$ and $\rho(\epsilon)$ is the electronic density of states for the transition. The different notations are graphically illustrated in Fig. 5 which represents a configurational diagram with two types of distortions and where, for convenience, we have arbitrarily assumed that $Q_\epsilon = 0$.

If we denote by E_T and E_0, respectively, the thermal energy and the optical threshold energy of the Cr^{2+} state with respect to the valence band, the following relations hold:

$$\begin{aligned}
\epsilon_i &= \tfrac{1}{2}k_A(Q_A^r)^2 + \tfrac{1}{2}k_E(Q_\theta^s)^2 + \tfrac{1}{2}k_E(Q_\epsilon^t)^2 , \\
\epsilon_f &= E_T + \tfrac{1}{2}k_A(Q_A^r - Q'_A)^2 + \tfrac{1}{2}k_E(Q_\theta^s - Q'_\theta)^2 \\
&\quad + \tfrac{1}{2}k_E(Q_\epsilon^t - Q'_\epsilon) + \epsilon , \\
E_0 &= E_T + \tfrac{1}{2}k_A(Q'_A)^2 + \tfrac{1}{2}k_E(Q'_\theta)^2 + \tfrac{1}{2}k_E(Q'_\epsilon)^2 \\
&= E_T + E_{\mathrm{rel}}^A + E_{\mathrm{rel}}^\theta + E_{\mathrm{rel}}^\epsilon ,
\end{aligned} \tag{4}$$

where E_{rel}^l is the relaxation energy given by l-type phonons.

Equation (3) can be written

$$\sigma(\hbar\omega) = A_i \int_{-\infty}^{+\infty} dQ_A^r \int_{-\infty}^{+\infty} dQ_\theta^s \int_{-\infty}^{+\infty} dQ_\epsilon^t [\chi_p^A(Q_A^r)\chi_m^E(Q_\theta^s)\chi_n^E(Q_\epsilon^t)]^2 \, \sigma_{\mathrm{el}} , \tag{5}$$

with

$$\sigma_{\mathrm{el}} = \frac{\mathfrak{C}}{\hbar\omega} \int_0^\infty d\epsilon\, \rho(\epsilon) M^2 \delta(E_0 + \epsilon - k_A Q'_A Q_A^r - k_E Q'_\theta Q_\theta^s - k_E Q'_\epsilon Q_\epsilon^t - \hbar\omega).$$

The next step averages over the initial p, m, and n states, and by the repetitive use of Mehler's formula and after some algebraic manipulations we have

$$\sigma(\hbar\omega) = \left(\frac{1}{\pi}\right)^{3/2} \int_{-\infty}^{+\infty} dX \int_{-\infty}^{+\infty} dY \int_{-\infty}^{+\infty} dZ\, \sigma_{\mathrm{el}}(E_0, \hbar\omega - \Gamma_A X - \Gamma_\theta Y - \Gamma_\epsilon Z)\, e^{-(X^2+Y^2+Z^2)} , \tag{6}$$

where $X^2 = (\xi_A Q_A^r)\tanh(\beta_A/2)$, $\xi_A = (k_A/\hbar\omega_A)^{1/2}$, and $\beta_A = \hbar\omega_A/kT$, with similar expressions for Y^2 and Z^2.

We have introduced the notations of Piekara *et al.*[19] for the broadening parameters Γ:

$$\begin{aligned}
\Gamma_A^2 &= 2\hbar\omega_A E_{\mathrm{rel}}^A \coth\frac{\beta_A}{2} , \\
\Gamma_\theta^2 &= 2\hbar\omega_E E_{\mathrm{rel}}^\theta \coth\frac{\beta_E}{2} , \\
\Gamma_\epsilon^2 &= 2\hbar\omega_E E_{\mathrm{rel}}^\epsilon \coth\frac{\beta_E}{2} .
\end{aligned} \tag{7}$$

and

σ_{el} contains explicitly a δ function and this limits the range of integration for X, Y, and Z to values

$$\Gamma_A X + \Gamma_\theta Y + \Gamma_\epsilon Z \leq \hbar\omega - E_0 .$$

To perform the integration, it is convenient to rotate the X, Y, Z axis in such a way that one of the new axes, say x, becomes perpendicular to the plane defined by $\Gamma_A X + \Gamma_\theta Y + \Gamma_\epsilon Z = \hbar\omega - E_0$. Then (6) becomes

$$\sigma(\hbar\omega) = \left(\frac{1}{\pi}\right)^{3/2} \int_{-\infty}^{+\infty} dy\, e^{-y^2} \int_{-\infty}^{+\infty} dz\, e^{-z^2} \times \int_{-\infty}^{\beta} dx\, e^{-x^2} \times \sigma_{\mathrm{el}}(E_0, \hbar\omega - \Gamma x)$$

or

$$\sigma(\hbar\omega) = \frac{\mathfrak{C}}{\hbar\omega}\frac{1}{\sqrt{\pi}} \int_{-\beta}^{\infty} dx\, e^{-x^2} \times \int_0^\infty d\epsilon\, M^2 \rho(\epsilon) \delta(E_0 + \epsilon + \Gamma x - \hbar\omega) , \tag{8}$$

where $\beta = (\hbar\omega - E_0)/\Gamma$ and from (7):

$$\begin{aligned}
\Gamma^2 = \Gamma_A^2 + \Gamma_\theta^2 + \Gamma_\epsilon^2 &= 2\hbar\omega_A E_{\mathrm{rel}}^A \coth\frac{\beta_A}{2} \\
&\quad + 2\hbar\omega_E E_{\mathrm{rel}}^E \coth\frac{\beta_E}{2} \\
&= \Gamma_A^2 + \Gamma_E^2 .
\end{aligned} \tag{9}$$

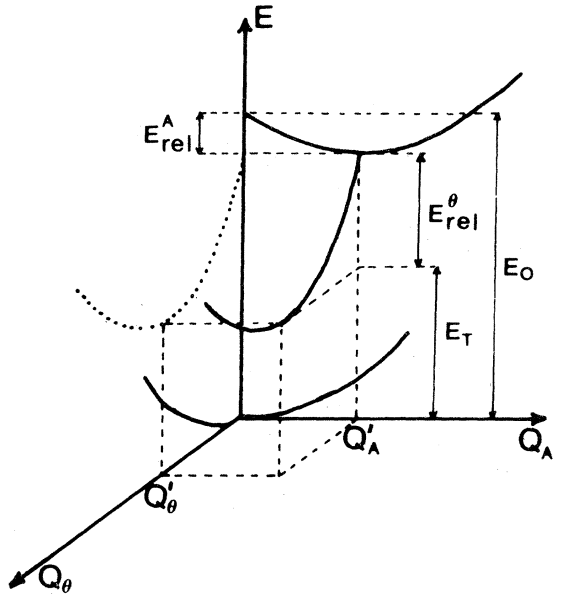

FIG. 5. Diagrammatic representation of a relaxation due to two different phonons: a symmetric one of A type and a nonsymmetric one of E type. For graphical convenience, we only sketched E^θ_{rel}. All parameters are defined in the text.

It is interesting to note that (8) is formally the same expression as that deduced by Piekara *et al.*[19] neglecting the E relaxation, but the interpretation of Γ (deduced by a fitting procedure) will be quite different.

B. Electronic model

To go beyond that point we need a model for describing the electronic transitions. We know that these transitions are allowed since there are p–d transitions, but there is no model to describe the d-wave functions inside the host crystal. On the other hand, the expression (8) already involves two fitting parameters E_0 and Γ, and it would not be reasonable to introduce other ones for which the fitting would not be sensitive.

The simplest model which does not introduce any extra parameter is the quantum defect model[20] in the limit of the Dirac potential (also called the Luckovsky's model[23]). With this model it is possible to calculate σ_{el} analytically, but the matrix element corresponds to p–s transitions and is then connected to the P parameter introduced by Kane.[24] This parameter is a function of the gap and of the effective masses. Following Bebb[20] and neglecting the nonparabolicity, we arrive at an expression for the photoionization cross section:

$$\sigma(\hbar\omega)=\frac{5.3\times10^{-14}}{n}\frac{E_G}{\hbar\omega}\frac{m}{m_c}\Gamma^{1/2}\left[E_0^{1/2}\int_{-\beta}^{\infty}dx\,e^{-x^2}(\beta+x)^{1/2}\left(\frac{\alpha_1^{1/2}}{[\hbar\omega+\Gamma x+E_0(\alpha_1-1)]^2}+\frac{\alpha_2^{1/2}}{[\hbar\omega+\Gamma x+E_0(\alpha_2-1)]^2}\right)\right.$$
$$\left.+(E_0+\Delta)^{1/2}\int_{-\beta_1}^{\infty}dx\,e^{-x^2}(\beta_1+x)^{1/2}\frac{\alpha_3^{1/2}}{[\hbar\omega+\Gamma x+(E_0+\Delta)(\alpha_3-1)]^2}\right], \tag{10}$$

where $\sigma(\hbar\omega)$ is given in cm^{-2} when all the energies are expressed in cm^{-1}. E_G is the energy gap, n the refractive index, and $\alpha_i=m/m_{vi}$, m, m_c, m_{v1}, m_{v2}, and m_{v3} being the free-electron mass, the conduction mass, and the three valence masses. Δ is the spin-orbit splitting.

In the expression (10) the three terms correspond to the different contributions of the three valence bands. Since the final electronic state is assumed to be of the s type, the three contributions from valence bands are only weighted by their respective density of states. For GaAs parameters, values of $\Gamma=650$ cm^{-1} and of $E_0=7450$ cm^{-1}, the three different contributions are drawn in Fig. 6. It is clear that the shape of the band depends strongly on the relative contributions of the heavy- and light-hole bands. In the fitting procedure performed by Kaminska *et al.*[17] for ZnSe, the electronic model was a two-band model with similar effective masses, corresponding here to the light-hole band. Then within this model the fitted values for Γ are necessarily too small.

VI. INTERPRETATION AND DISCUSSION OF THE ABSORPTION RESULTS

A. Structure of the absorption as a function of the energy

Figure 6 shows that the model [Eq. (10)] does not predict any irregularity other than that which appears beyond 9600 cm^{-1} and which is due to the spin-orbit split valence band. In the range of 8600 cm^{-1} nothing happens in contradiction with the experimental results (Fig. 2), so it is clear that another transition occurs at an energy E_0' higher than E_0. The simplest solutions are those involving either a lower initial state or higher final state for the transition.

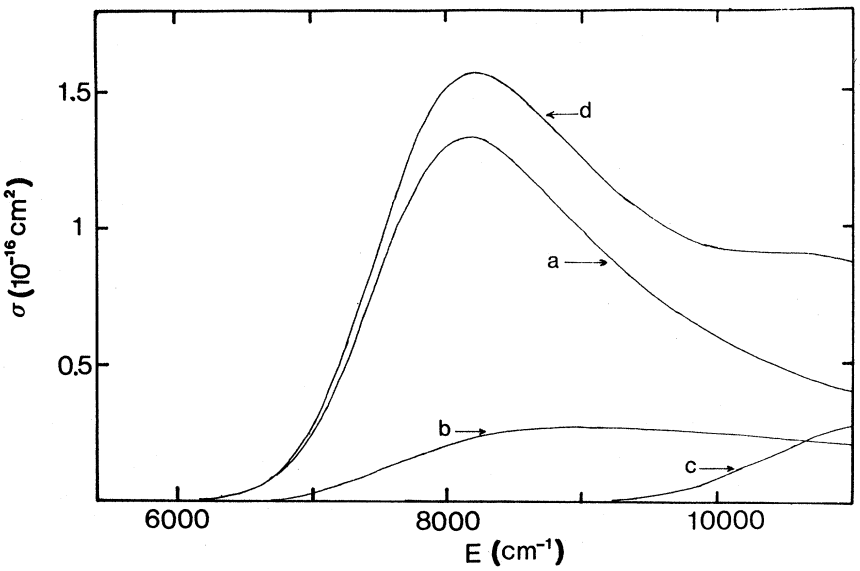

FIG. 6. Results of the theoretical model given by Eq. (10) for GaAs parameters and with $\Gamma = 650\ cm^{-1}$, $E_0 = 7450\ cm^{-1}$ (a) heavy-hole band contribution, (b) light-hole band contribution, (c) spin-orbit split hole band contribution, (d) sum of the (a), (b), and (c) contributions.

The former alternative could be understood since, working with deep impurities, their levels are spread in the Brillouin zone and it is not obvious that the transitions originate from the Γ point. If we go away from this point in the Brillouin zone, the light- and heavy-hole bands are split and the difference between E_0' and E_0 could be due to this splitting, the light-holes contribution in Fig. 6 being shifted with respect to the heavy-holes contribution. This possibility is hard to rule out. One argument against it is that such an effect should have been seen in ZnSe:Cr (Ref. 17), which it was not. Finally, such a model would lead us to introduce extra fitting parameters in the expression (10) for the effective masses which would have different values than those for the band edge.

The second possibility that we have finally chosen is to assume a higher final-energy state than the fundamental state of Cr^{2+}. This possibility which does not exist in II–VI compounds since the lower level of the final state (Cr^{1+}) is of $^6A_1$ symmetry, is offered in our case by the splitting, due to the Jahn-Teller effect, of the fundamental level $^5T_2$ of Cr^{2+} into a $^5B_2$ (fundamental) and ^5E levels (see paper II). In the Cr^{2+} stable configuration (D_{2d} symmetry), these levels are split by three times the Jahn-Teller energy $\mathcal{E}_{\mathrm{JT}}^{T_2}$. But the final state of the present transition is different from these levels in many aspects: Besides the symmetrical distortion introduced by the extra electron, the final-state levels are those of a $3d^4$ electronic configuration in a C_{2v} symmetry state which splits the ^5E level into two levels, and the relaxation towards the D_{2d} symmetry involves E as well as T_2 phonons. This is a very hard problem to solve and we are then led to make further assumptions: (i) We shall postulate that the symmetrical distortion is the same for the fundamental and excited levels of the final states. This is quite reasonable since the number of electrons is the same for both levels. (ii) Once this distortion is taken into account, we are left with a $T_2 + E$ problem for which the potential part of the Hamiltonian of interaction can be written as[25]

$$\mathcal{H}_{\mathrm{int}}^{V} = V_E(Q_\theta \mathcal{E}_\theta + Q_\epsilon \mathcal{E}_\epsilon) + V_{T_2}(Q_\xi \mathcal{T}_{2\xi} + Q_\eta \mathcal{T}_{2\eta} + Q_\zeta \mathcal{T}_{2\zeta}), \tag{11}$$

which acts on the fundamental $^5T_2$ levels of the electronic state of Cr^{2+}. V_E, V_{T_2} are the Jahn-Teller coupling coefficients for the E and T_2 modes, Q_θ, Q_ϵ the coordinates for the E mode, and Q_ξ, Q_η, Q_ζ are those for the T_2 modes. $\mathcal{E}_\theta$, $\mathcal{E}_\epsilon$ and $\mathcal{T}_{2\xi}$, $\mathcal{T}_{2\eta}$, $\mathcal{T}_{2\zeta}$ are, respectively, the electronic operators for the E and T_2 modes. It turns out that the $\mathcal{E}$ operators are diagonal in the basis of the $^5T_2$ level whereas the $\mathcal{T}_2$ operators are nondiagonal in this basis. As this has been shown by Ham,[25] this difference induces a partial quenching of the last term proportional to V_{T_2} in Eq. (11) with respect to the first one proportional to V_E.

We shall assume that this quenching is sufficiently efficient to reduce $\mathcal{H}_{\mathrm{int}}^{V}$ only to the V_E-dependent

term. With this approximation the adiabatic potential-energy surfaces are the same as those involved in the Jahn-Teller effect of Cr^{2+} (see paper II) and described by Sturge.[26] They are made of three identical paraboloidal sheets rotated one with respect to the other by $\pm 2\pi/3$. So within this approximate model the surfaces are known but the distortion (Q_θ, Q_ϵ) corresponding to the final state of the optical transition is not.

Öpik and Pryce[27] have studied a similar situation for an octahedral coordination and have shown that in the case of an intermediate distortion (between tetragonal and trigonal), the corresponding Q_ϵ distortion is zero. That corresponds to our taking the second final state of the transition as two-fold degenerated. In fact, our fitting procedure will not be sensitive to an eventual splitting of these levels by less than 100 cm^{-1}.

We now try to interpret the experimental results with the model described by Eq. (10). This model depends on two independent parameters, Γ and E_0. We add to it a second contribution formally identical to Eq. (10) (but multiplied by 2 to take into account the degeneracy) shifted in energy to E_0', with a value Γ' different from Γ. In the model we choose to reproduce the experiment, the thermal energy E_T, after the relaxation, is the same for the E_0 and E_0' transitions, and then Γ and Γ' are not independent. Using Eq. (9) it comes out that

$$\Gamma'^2 = \Gamma^2 + 2\hbar\omega_E (E_0' - E_0)\coth\frac{\beta_E}{2} . \tag{12}$$

We shall use to interpret Γ^2 (see below) the value of $\hbar\omega_E = 82$ cm^{-1} which is that found for Cr^{2+} (see paper II). So with that assumption and the help of Eq. (12), we are left with only three fitting parameters: E_0, E_0', and Γ and a fourth one which determines the strength of the absorption. It turns out that with all these assumptions, the fit is sufficiently poor to raise the question of the validity of the model for electronic transitions included in Eq. (10). In fact, we are looking at p–d transitions and the matrix elements for transitions between the three valence bands and the $^5T_2$ and ^5E levels are not the same. It is easy to show that with the wave functions for valence bands given by Kane[24] and those of $^5B_2$ and ^5E levels given by Ham,[25] the average of the square of the matrix elements between these different levels is such that (i) for the first transition (E_0) to the $^5B_2$ level, the contribution from the heavy-hole band has to be multiplied by 1, that from the light-hole band by $\frac{1}{3}$, and that from the spin-orbit split band by $\frac{2}{3}$. (ii) For the second transition E_0' to the ^5E level, the contribution from the heavy-hole band has to be multiplied by $\frac{1}{2}\times 2$, that from the light-hole band by $\frac{3}{2}\times 2$, and that from the spin-orbit split band by $\frac{2}{3}\times 2$, where the factor 2 takes care of the degeneracy of the band.

So the final expression used to fit the experimental results is

$$\sigma(\hbar\omega) = \frac{5.3\times 10^{-14}}{n}\frac{E_G}{\hbar\omega}\frac{m}{m_c}(\sigma_1 + \sigma_2) ,$$

with

$$\sigma_1 = \Gamma^{1/2}\left[E_0^{1/2}\int_{-\beta}^{\infty} dx\, e^{-x^2}(\beta + x)^{1/2}\left(\frac{\alpha_2^{1/2}}{[\hbar\omega + \Gamma x + E_0(\alpha_1 - 1)]^2} + \frac{\alpha_2^{1/2}}{3[\hbar\omega + \Gamma x + E_0(\alpha_2 - 1)]^2}\right)\right.$$
$$\left. + (E_0 + \Delta)^{1/2}\int_{-\beta_1}^{\infty} dx\, e^{-x^2}(\beta_1 + x)^2 \frac{2\alpha_3^{1/2}}{[\hbar\omega + \Gamma x + (E_0 + \Delta)(\alpha_3 - 1)]^2}\right] \tag{13}$$

and

$$\sigma_2 = \Gamma'^{1/2}\left[E_0'^{1/2}\int_{-\beta'}^{\infty} dx\, e^{-x}(\beta' + x)^{1/2}\left(\frac{\alpha_1^{1/2}}{[\hbar\omega + \Gamma' x + E_0'(\alpha_1 - 1)]^2} + \frac{3\alpha_2^{1/2}}{[\hbar\omega + \Gamma' x + E_0'(\alpha_2 - 1)]^2}\right)\right.$$
$$\left. + (E_0' + \Delta)^{1/2}\int_{-\beta_1'}^{\infty} dx\, e^{-x^2}(\beta_1' + x)^2 \frac{4\alpha_3^{1/2}}{3[\hbar\omega + \Gamma' x + (E_0' + \Delta)(\alpha_3 - 1)]^2}\right].$$

This does not take into account the difference between the radial part of a p–s matrix element and that of a p–d matrix element, the evaluation of which would require the knowledge of the extent of the d-wave function of the chromium impurity in the host GaAs lattice. So, the model we have chosen keeps the radial part of the matrix elements identical to that of a p-s transition, but modulates the different contributions of the Eq. (10) with the factors coming from the angular part of the matrix elements.

The results of the fitting procedure are shown as solid lines in Figs. 1–3. The strength of the absorption is fit at 4.5 K (Fig. 2) where the different contributions coming from the E_0 and E_0' transitions [σ_1 and σ_2 in Eq. (13)] are detailed. This gives us the number of Cr^{3+} centers if the absolute value of the cross section given by Eq. (13) is cor-

rect. This will be discussed in Sec. VID. This value has of course been kept constant for other temperatures and pressures.

There remains some discrepancy around 7300 and 8000 cm^{-1}. The first one is probably due to the presence of a small number of Cr^{2+} charge states which develop some extra absorption (see paper II) in this region. The second discrepancy at 8000 cm^{-1} seems irreducible within our model. It may be due to the approximation of the evaluation of the radial part of the matrix elements or (and) to the fact that we neglect the nonparabolicity in the model. This discrepancy is less apparent at higher temperatures but still exists.

However, the relative strength which varies with Γ and E_0 through Eq. (13) is in accordance with the experimental results as a function of the temperature or the pressure. The precision of the fitting is not sufficient to measure either a significant change of E_0 (or E_0') with temperature or a change of Γ with pressure as this is shown in Table II when all results are gathered.

B. Absorption as a function of the temperature

With the interpretation of the temperature variation of Γ it is possible to deduce the different parameters entering Eq. (9). However, we need to make at least one further assumption on $\hbar\omega_A$ or $\hbar\omega_E$. Γ^2 varies with temperature as sketched on Fig. 7 starting at $T=0$ K at a value of $2\hbar\omega_A E^A_{rel} + 2\hbar\omega_E E^E_{rel}$, and reaches asymptotically with temperature the line $\Gamma^2 = 4(E^A_{rel} + E^E_{rel})kT$. In principle, since $E^A_{rel} + E^E_{rel} = E_0 - E_T$, E_0 is fit (Table II) and E_T known,[28,29] we only need to know $\hbar\omega_A$ or $\hbar\omega_E$ to deduce all other parameters. We assume that the total relaxation energy is temperature independent and that $\hbar\omega_E = 82$ cm^{-1}, which is the value of the E phonon found for the relaxation of intracenter transitions within the Cr^{2+} levels (see paper II). Unfortunately, this assumption is not sufficient because with the combined experimental errors in Γ (Table II) and E_T,[28,29] the values found for $\hbar\omega_A$ spread too large a range of energies.

The expression (9) can be written at low temperature as

TABLE II. Fitted parameters entering Eq. (13) for different temperatures and pressures.

T (K)	P (bar)	E_0 (cm^{-1})	E_0' (cm^{-1})	Γ (cm^{-1})
4.5	1	7400 ± 25	8450 ± 25	725 ± 25
77	1	7400 ± 25	8450 ± 25	750 ± 25
77	9250	7625 ± 25	8675 ± 25	750 ± 25
300	1	7400 ± 25	8450 ± 25	1125 ± 25
300	9250	7625 ± 25	8675 ± 25	1125 ± 25

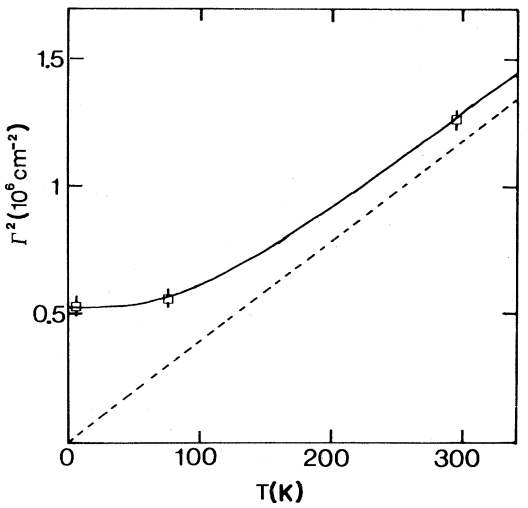

FIG. 7. Variation of the broadening parameter with temperature. The solid line reproduces the variation given by Eq. (9) with the set of parameters given in the text. Empty squares are the experimental values (Table II). The dashed line is the asymptotic behavior of Eq. (9).

$$\Gamma^2(4\text{ K}) = (2\hbar\omega_E E^E_{rel} + \hbar\omega_A E^A_{rel}), \tag{14}$$

and by expanding the hyperbolic function at high temperatures (≃300 K) as

$$3kT\Gamma^2(300\text{ K}) = 12(kT)^2(E^E_{rel} + E^A_{rel}) + (\hbar\omega_E)^2 E^E_{rel} + (\hbar\omega_A)^2 E^A_{rel}. \tag{15}$$

It is possible, using the model adopted for the transitions, to overcome the difficulty due to the experimental uncertainty. The difference between the optical thresholds $E_0' - E_0 = \Delta E$ can be related to the relaxation energy E^E_{rel}. It is easy to show, writing the equations for the adiabatic potential-energy surfaces of the $^5B_2$ and ^5E levels, that the following relation holds:

$$\frac{4\Delta E}{\mathcal{E}^{T_2}_{JT}} = \frac{[3 - (12\alpha + 9)^{1/2}]^2}{\alpha}, \tag{16}$$

with $\alpha = \Delta E / E^E_{rel}$. If we know experimentally ΔE and the limiting values of the Jahn-Teller energy $\mathcal{E}^{T_2}_{JT}$, the solution of (16) gives α and then E^E_{rel}. This procedure is much less sensitive to experimental errors. As will be discussed in paper II, the Jahn-Teller energy of the ^5E excited level is probably very weak and then $\mathcal{E}^{T_2}_{JT}$ should be of the order of 660 cm^{-1}. The solution of (16) corresponds to $E^E_{rel} = 146$ cm^{-1}. With this value, all other parameters are deduced from Eqs. (14) and (15). The main error comes now from the uncertainty of Γ(300 K): we get $E^A_{rel} = 1310 \pm 50$ cm^{-1} and $\hbar\omega_A = 190 \pm 10$ cm^{-1}. The thermal energy is then $E_T = E_0 - E^A_{rel} - E^E_{rel} = 5940 \pm 50$ cm^{-1}.

The relaxation due to the E mode is found to be much smaller than E_{rel}^{A}. This small value corresponds in the Q_θ plane to an E distortion of the Cr^{3+} level, significantly smaller than that of the Cr^{2+} level, and it is easy to calculate the ratio of these two different distortions: $Q_\theta(Cr^{3+})/Q_\theta(Cr^{2+}) \simeq 0.5$. The small value of E_{rel}^{E} (with respect to $\mathcal{E}_{JT}^{T_2}$) reflects this difference. If we are dealing with transitions from a d to an s state like in ZnSe:Cr, the relative weight of E^E with respect to E^A could be larger than here. The E_0 an E_T values fit quite well with those reported in the literature from photocapacitance measurements[30] and galvanomagnetic measurements.[28,29] The value for $\hbar\omega_A$ corresponds to a peak in the density of states of GaAs, due in part to the LA phonons of L_1 symmetry. In the cluster model which is the basis of the configurational-diagram approach, the A mode can be generated by the host-lattice phonons of symmetry X_1 or L_1 and then from a symmetry point of view, the results are coherent. However, in ZnS doped with transition-metal impurities (including chromium), the A-type localized mode lie[31] within the optical-phonon density of states of the host lattice. That would correspond for GaAs to values higher than 230 cm^{-1}.

C. Absorption as a function of pressure

As we have already pointed out, the precision of the fit does not allow us to see a significant change of Γ with pressure. Since the phonon energies do not vary much with pressure, this result would predict a small variation of the relaxation energy and of the Jahn-Teller effect as a function of the pressure. Through this does not contradict similar results found in Al_2O_3:Cr (Ref. 32), it is worth pointing out that, due to our uncertainty of Γ, the upper limit of variation, with pressure, for E_{rel} is found to be rather large (2×10^{-6} eV/bar).

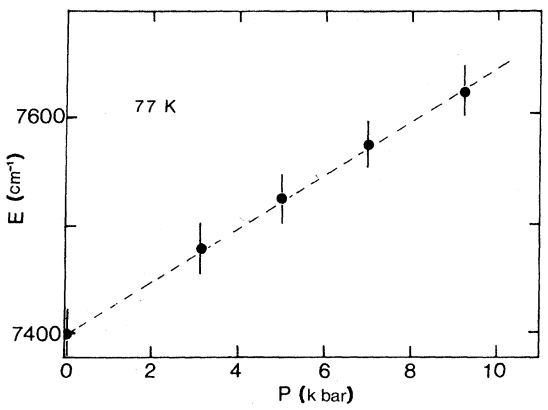

FIG. 8. Variation of E_0 with pressure at 77 K.

The experiment is more sensitive to the change of E_0 or E_0' with the pressure. The variation of E_0 is shown in Fig. 8 at 77 K. We find that $\partial E_0/\partial P \simeq \partial E_0'/\partial P = 3 \pm 0.7\times10^{-6}$ eV/bar. This coefficient agrees reasonably well with the value $2.1 \pm 1\times10^{-6}$ eV/bar obtained by White *et al.*[33] from capacitance measurements. From these results the upper limit of variation of $\Delta E = E_0 - E_0'$ with pressure is found to be 0.5×10^{-6} eV/bar. Since Γ does not vary with pressure, this last result corresponds also to an upper limit of the variation of the Jahn-Teller energy $\mathcal{E}_{JT}^{T_2}$ with pressure. So in a first approximation, the measured variation of E_0 (or E_0') can be assigned to that of the $^5T_2$ level of the Cr^{2+} with respect to the valence band of the host lattice.

D. Absolute value of the cross section

This value is obtained experimentally since we know (Table I) the chromium concentration of the Cr_8 sample. We obtain $\sigma \simeq 9\times10^{-17}$ cm^{-2} at 9000 cm^{-1}. This corresponds quite well to the calibration given by Martin *et al.*[6] The comparison between this value and the calculated one through Eq. (13) is not easy. We found at 9000 cm^{-1} that $\sigma_{calc} = 1.5\times10^{-17}$ cm^{-2}, a result which includes the value of the radial part of the p–s matrix elements instead of the p–d one. It is then difficult to discuss the difference between these two values since the evaluation of the p–d matrix element would require the knowledge of the extension of the d functions in the host lattice, information which is missing.

VII. EPR RESULTS AND DISCUSSION

Up to now, three EPR spectra, characteristic of chromium in GaAs, are reported in the literature: one due to the Cr^{3+} (Ref. 34), one due to Cr^{2+} (Ref. 10), and a third one characterized by $g = 1.993$ (Ref. 35) or $g = 1.995$ (Ref. 10) and a linewidth of 115 G.

The Cr^{3+} signal is dominant in the Cr_8 sample (Fig. 4) and decreases noticeably with the 1.09-μm light illumination of the sample whereas the Cr^{2+} signal increases. From this experiment we can deduce the ratio of the EPR sensitivity of the Cr^{3+} to Cr^{2+} which is found to be of the order of two in our experiments, but which is strongly dependent on temperature and internal strains as pointed out by Stauss *et al.*[36] The Cr^{3+} signal is also found in the Cr_4, Cr_5, Cr_6, and Cr_7 samples though it is no longer dominant. This fact will be used in paper II for the interpretation of experimental data. In the Cr_1, Cr_2, and Cr_3 samples, the very large cyclotron resonance signal prevents any observation of this signal.

The Cr^{2+} signal is dominant for n-type samples and its behavior under illumination is such that this signal never decreases. For the Cr_1, Cr_2, and Cr_3 samples the signal is invariant, whereas it increases from 10% (Cr_4) to 30% (Cr_7) with an increase rate which can be correlated at least qualitatively to the increasing number of residual Cr^{3+} centers

The $g=1.993$ signal is observed in all our samples and always increases under 1.09-μm light. This signal was first attributed to Cr^+ (Refs. 35 and 10). But, even assuming a large degree of inhomogeneity in the samples, it is hard to conceive that such a state would still be stable in a p-type sample. Moreover, the attribution of this signal to Cr^+ is in contradiction with our results (see paper II) where this level is shown to be degenerated with the conduction band by an amount of about 60 meV. In order to have the Fermi level higher than this Cr^{2+} level, one should have a carrier concentration higher than 10^{19} cm^{-3}, i.e., one order of magnitude larger than the electron concentration in the Cr_0 sample. In this respect, the recent assumption[11,37] that this signal could be due to Cr^{4+} seems much more plausible.

It remains that the three different EPR signals are observed in the same samples. If this situation in p-type samples can be understood, it is not clear for n-type samples without assuming a variation of the chromium doping within each sample. The analysis of EPR spectra as well as SIMS measurements of different parts of the same sample shows indeed a variation of the chromium concentration within a factor 2. The same kind of inhomogeneities have also been observed in samples doped during the melt. So, it is likely that the chromium doping itself gives rise to a certain amount of chromium "aggregates" in the samples.

Besides these chromium characteristic lines, the only EPR signal observed in our samples is that of Fe^{3+}, the intensity of which is sample dependent. It is even seen in the Cr_0 sample. The dependence of the strength of this signal with samples has to be related to the variation of the Fermi level and probably not to a variation of the iron doping in the different samples. This observation correlates the impurity measurements discussed in Sec. II.

VIII. CONCLUSION

This report on the photoionization process of the chromium impurity in GaAs shows that the interpretation of experimental results requires the concept of optical transitions between vibronic states. A model using this concept has been developed and involves transitions from the different valence bands coupled to two kinds of phonons. The comparison with the experimental data shows that the relaxation of the center by E-type phonons is weaker than that due to A-type phonons. Additional information is obtained for the relative distortion of the Cr^{3+} charge state with respect to the Cr^{2+} one. The phonons assisting these relaxations are found to be in a range of high phonon density of states of the host lattice.

ACKNOWLEDGMENTS

We are very grateful to Dr. G. Poiblaud (RTC, Caen) who has kindly provided us the ingot of n-type GaAs used for the diffusion of chromium, to Dr. M. Kaminska for her help in our computer calculations, and to Professor J. Schneider and Dr. U. Kaufmann for making their results available prior to publication. This work was supported in part by DGRST under Contract No. 78-7-0307.

---

*On leave from the Institute of Experimental Physics, Warsaw University, Warsaw, Poland.

[1]W. H. Koschel, S. G. Bishop, and B. D. McCombe, Solid State Commun. 19, 521 (1976).

[2]T. Instone and L. Eaves, J. Phys. C 11, L771 (1978).

[3]K. Kocot, R. A. Rao, and G. L. Pearson, Phys. Rev. B 19, 2059 (1979).

[4]V. V. Ushakov, A. A. Gippius, and B. V. Kornilov, Fiz. Tekh. Poluprovodn. 12, 358 (1978) [Sov. Phys.–Semicond. 12, 207 (1978)].

[5]D. Bois and P. Pinard, Phys. Rev. B 9, 4171 (1974).

[6]G. M. Martin, M. L. Verheitke, J. A. A. Jansen, and G. Poiblaud, J. Appl. Phys. 50, 467 (1977).

[7]J. T. Vallin and G. D. Watkins, Phys. Rev. B 9, 2051 (1974).

[8]J. T. Vallin, G. A. Slack, S. Roberts, and A. E. Hughes, Phys. Rev. B 2, 4313 (1970).

[9]M. Kaminska, J. M. Baranowski, S. M. Uba, and J. T. Vallin, J. Phys. C 12, 2797 (1979).

[10]J. J. Krebs and G. H. Stauss, Phys. Rev. B 16, 971 (1977).

[11]U. Kaufmann and J. Schneider, Appl. Phys. Lett. 36, 747 (1980).

[12]A. M. Hennel, W. Szuszkiewicz, M. Balkanski, G. Martinez, and B. Clerjaud, following paper, Phys. Rev. B 23, 3933 (1980).

[13]N. Dahan, B. Barrau, G. Pinzutti, and G. Martinez (unpublished).

[14]B. Clerjaud and B. Lambert, J. Phys. E 4, 619 (1971).

[15]C. E. Jones and A. R. Hilton, J. Electrochem. Soc. 113, 504 (1966).

[16]G. K. Ippolitova, E. M. Omel'Yanovskii, and L. Ya Perwowa, Fiz. Tekh. Poluprovodn. 9, 1308 (1975) [Sov. Phys.—Semicond. 9, 864 (1976)].

[17]M. Kaminska, J. M. Baranowski, and M. Godlewski, in *Proceedings of the 14th International Conference on*

the Physics of Semiconductors, (The Institute of Physics, Bristol and London, 1979), p. 303.
[18]U. Piekara, J. M. Langer, B. Krukowska Fulde, Solid State Commun. 23, 583 (1977).
[19]J. W. Allen, J. Phys. C 2, 1077 (1969).
[20]H. B. Bebb, Phys. Rev. 185, 1116 (1969).
[21]A. A. Kopylov and A. N. Pikhtin, Fiz. Tverd. Tela 16, 1837 (1974) [Sov. Phys.–Solid State 16, 1200 (1975)].
[22]M. Lax, J. Chem. Phys. 20, 1752 (1952).
[23]G. Lucovsky, Solid State Commun. 3, 299 (1965).
[24]E. O. Kane, J. Phys. Chem. Solids 1, 249 (1957).
[25]F. S. Ham, Phys. Rev. 138A, 1727 (1965).
[26]M. D. Sturge, in *Solid State Physics*, edited by F. Seitz and D. Turnbull (Academic, New York, 1967), Vol. 20, p. 153.
[27]U. Öpik and M. H. L. Pryce, Proc. R. Soc. London, 238, 425 (1957).
[28]R. W. Haisty and G. R. Cronin, in *Proceedings of the 7th International Conference on the Physics of Semiconductors* (Dunod, Paris, 1964), p. 1161.
[29]G. A. Allen, Br. J. Appl. Phys. 2, 593 (1968).
[30]K. Kocot and M. Kaminska (unpublished).
[31]M. Zigone, K. Kunc, P. Plumelle, and M. Vandevyver, in *Proceedings of the International Conference on Lattice Dynamics, Paris, 1977,* edited by M. Balkanski (Flammarion, Paris, 1978), p. 405.
[32]S. Minomura and H. G. Drickamer, J. Chem. Phys. 35, 903 (1961).
[33]A. M. White, P. Porteous, W. F. Sherman, and A. A. Stadtmuller, J. Phys. C 10, L473 (1977).
[34]J. J. Krebs and G. H. Strauss, Phys. Rev. B 15, 17 (1977).
[35]U. Kaufmann and J. Schneider, Solid State Commun. 20, 143 (1976).
[36]G. H. Stauss, J. J. Krebs, S. H. Lee, and E. M. Swiggard, J. Appl. Phys. 50, 6251 (1979).
[37]G. H. Stauss, J. J. Krebs, S. H. Lee, and E. M. Swiggard, Phys. Rev. B 22, 3141 (1980).